18PB-087

Relativistic baroclinic effect in electron two fluid plasma

電子二流体における相対論的傾圧効果

Yohei Kawazura and Zensho Yoshida

川面洋平，吉田善章

Graduate School of Frontier Sciences, University of Tokyo
5-1-5 Kashiwanoha, Kashiwa, Chiba 277-8561, Japan
東京大学新領域創成科学研究科 〒 *277-8561* 千葉県柏市柏の葉 *5-1-5*

We investigate the relativistic baroclinic effect by three dimensional electron two fluid plasma simulation with the parameters relevant for high intensity laser experiments. Due to the return current by cold electrons, highly relativistic plasma is sustained for long time. The observed relativistic baroclinicity is more than twice larger than conventional thermal baroclinic effect. Although the spacial structure of the thermal and relativistic baroclinic terms are identical on shock front surface, the separation of spatial structure is observed in post shock region, and amplitude ratio is larger than that on the shock front.

1 Introduction

It has been a big mystery how the seed (primordial) magnetic field is generated in the universe. In fluid description of plasma, magnetic field is coupled with mechanical vorticity, then represented as curl of canonical vorticity $\boldsymbol{P} = m\boldsymbol{V} + q\boldsymbol{A}$, where $\boldsymbol{V}$ and $\boldsymbol{A}$ are fluid velocity and vector potential, m is the mass of the particles and q is the charge. The time evolution of $\boldsymbol{P}$ is written as

$$\partial_t \boldsymbol{P} + (\nabla \times \boldsymbol{P}) \times \boldsymbol{V} = -\nabla\left(\frac{mV^2}{2} + h + q\phi\right) + T\nabla\sigma,$$

where ϕ denotes electrostatic potential, T is the temperature and σ is the specific entropy. The only available term to generate magnetic field is $\nabla T \times \nabla\sigma$ which is called thermal baroclinic term. However the preceding work in astrophysics elucidated that thermal baroclinic effect cannot generate seed magnetic field enough to be grown to the present field [1]. The early universe was almost thermal equilibrium, which is why the baroclinic term was supposed to be weak.

Mahajan and Yoshida proposed a novel mechanism of vorticity generation by relativistic effect [2, 3]. The relativistic equation of motion in the reference frame is written as

$$\partial_t \boldsymbol{P} + (\nabla \times \boldsymbol{P}) \times \boldsymbol{V} = -\nabla\left(h\gamma + q\phi\right) + \frac{T}{\gamma}\nabla\sigma,$$

where γ denotes the Lorentz factor. In addition to the thermal baroclinicity ($\boldsymbol{S}_\mathrm{T} = \gamma^{-1}\nabla T \times \nabla\sigma$), there appears "relativistic baroclinic term" $\boldsymbol{S}_\mathrm{R} = T\nabla\gamma^{-1} \times \nabla\sigma$. This new term has potential to generate seed magnetic field because even in almost thermal equilibrium $\boldsymbol{S}_\mathrm{R}$ can be finite.

Our next step is to verify the relativistic baroclinic effect experimentally. Recent progress in high intensity laser experiments enables us to obtain relativistic electron plasma, and some of the preceding works showed the measurement of generated magnetic field in high accuracy [4]. The relativistic baroclinicity is expected to be verified in such high intensity laser experiments. In this study, we conduct numerical simulations of electron plasma with the parameters relevant for laser experiments. In the typical time scale of these experiments, the ions are assumed to be immovable. The high γ state is realized by charge neutralization due to the return current of cold electrons, otherwise the drag force by the electric field reduces γ significantly. Therefore our simulation model consists of hot and cold two components electron fluid.

2 Basic equations

We calculate nonlinear evolution of two temperature electron fluid and Maxwell's equations:

$$\partial_t N_\mathrm{h,c} + \nabla \cdot (N_\mathrm{h,c}\boldsymbol{v}_\mathrm{h,c}) = 0$$
$$\partial_t \boldsymbol{M}_\mathrm{h,c} + \nabla \cdot (\boldsymbol{M}_\mathrm{h,c}\boldsymbol{v}_\mathrm{h,c} + p_\mathrm{h,c}\mathsf{I}) = -N_\mathrm{h,c}(\boldsymbol{E} + \boldsymbol{v}_\mathrm{h,c} \times \boldsymbol{B})$$
$$\partial_t \mathcal{E}_\mathrm{h,c} + \nabla \cdot [(\mathcal{E}_\mathrm{h,c} + p_\mathrm{h,c})\boldsymbol{v}_\mathrm{h,c}] = -N_\mathrm{h,c}\boldsymbol{E} \cdot \boldsymbol{v}_\mathrm{h,c}$$
$$\partial_t \boldsymbol{B} + \nabla \times \boldsymbol{E} = 0$$
$$\partial_t \boldsymbol{E} - \nabla \times \boldsymbol{B} - \epsilon^{-2}(N_\mathrm{h}\boldsymbol{v}_\mathrm{h} + N_\mathrm{c}\boldsymbol{v}_\mathrm{c}) = 0,$$

where $N = n\gamma$ (n : rest number density), $\boldsymbol{M} = Nh\gamma\boldsymbol{v}$, $\mathcal{E} = Nh\gamma - p$ (p : pressure), I is the unit tensor, $\boldsymbol{E}$ is the electric field, and $\boldsymbol{B}$ is the magnetic field. The indices h and c represent hot and cold component respectively. The variables are normalized as $\boldsymbol{v} \to \boldsymbol{v}/c$, $\boldsymbol{x} \to \boldsymbol{x}/L$, $t \to t/(L/c)$, $\boldsymbol{B} \to \boldsymbol{B}/(mc^2/Lq)$ and $\boldsymbol{E} \to \boldsymbol{E}/(mc^2/Lq)$, where c is the speed of light, L is characteristic scale length, m is the electron mass and q is the elementary charge. The scale parameter ϵ is given as $\sqrt{mc^4/4\pi q^2 n_0}/L$. We assume ideal gas ($h = 1 + \Gamma p/(\Gamma - 1)n$, $\Gamma = 4/3$).

3 Numerical simulation

Figure 1 illustrates the initial configuration. Hot and cold electron fluid are separated by different contact surfaces for the density and the temperature. Temperature discontinuity is located at $z = -0.6$. For $z < -0.6$, temperature of hot/cold electron is denoted as $T_{\rm h}^0/T_{\rm c}^0$, and $T_{\rm h}^1/T_{\rm c}^1$ for $z > -0.6$. Density discontinuity is located at $z = -0.2$ and perturbed with amplitude of 0.2 along z direction and 0.1 along $x-y$ direction randomly. In the same way as the temperature discontinuity, we denotes the density of hot/cold electron before and after discontinuity as $n_{\rm h}^0/n_{\rm c}^0$ and $n_{\rm h}^1/n_{\rm c}^1$. We set the initial density as $n_{\rm h}^1 = \alpha n_{\rm h}^0$, $n_{\rm c}^0 = 1.0 - n_{\rm h}^0$ and $n_{\rm c}^1 = 1.0 - n_{\rm h}^1$, and the initial temperature as $T_{\rm h}^1 = \beta T_{\rm h}^0$ and $T_{\rm c}^0 = T_{\rm c}^1 = T_{\rm h}^1$. Marquina's relativistic flux split algorithm

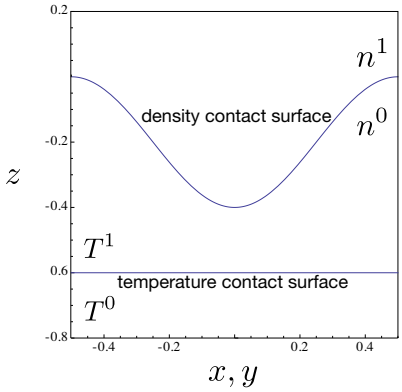

Fig. 1 Initial configuration

is used for solving the equation of motion [5]. The spacial accuracy is second order by MUSCL interpolation. The time integral is third order TVD Runge-Kutta method.

We show the result of the simulation for $n_{\rm h}^0 = 0.9$, $\alpha = 10^{-3}$, $T_{\rm h}^0 = 2.0\,(\sim 1\,\mathrm{MeV})$, $\beta = 10^{-2}$ and $\epsilon^{-2} = 20$ (corresponding physical parameter region is $n_0 \sim 10^{21}\,/\mathrm{cm}^3$ and $L \sim 10\,\mu\mathrm{m}$). The simulation is conduct up to $t = 20$. The simulation box moves along z direction with v_z at $z = 0$, which is equivalent to the velocity of shock front. Figure 2 is snapshots of rest density distribution. Initially Richtmyer-Meshkov instability occurs then density is stirred. Due to the return current by cold electron, highly relativistic state is sustained for entire calculation time. By decreasing α, corresponding to decreasing two fluidness, hot electron's velocity becomes non relativistic. We investigate the baroclinic effect in the final state. The norm of $\boldsymbol{S}_{\rm R}$ and $\boldsymbol{S}_{\rm T}$ on z-slice is depicted in Fig. 2. On $z = 0.0$ slice, which corresponds to the shock front surface, the baroclinic terms form filament like structure. The amplitude of $|\boldsymbol{S}_{\rm R}|$ is twice larger than $|\boldsymbol{S}_{\rm T}|$. Both terms are spatially identical except for near the center. On $z = -1.5$ slice, post shock region, baroclinicities are 10^{-3} smaller than those on $z = 0.0$ slice. However $|\boldsymbol{S}_{\rm R}|$ and $|\boldsymbol{S}_{\rm T}|$ have different spacial structure, and amplitude ratio is around sixth. From these observations, the characteristics of relativistic baroclinicty is observable in post shock region.

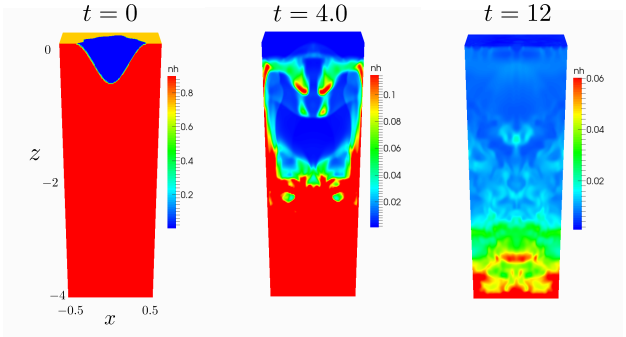

Fig. 2 Three dimensional density evolution

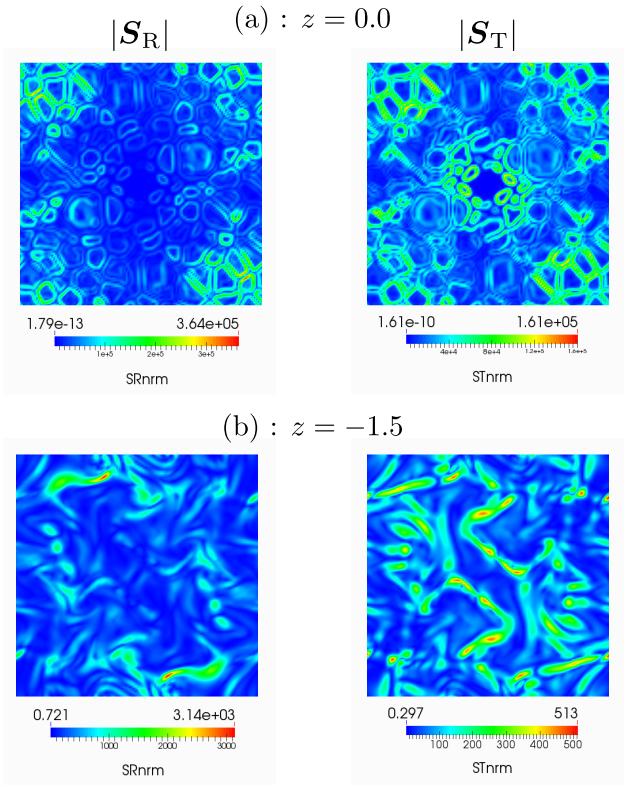

Fig. 3 Spatial profiles of $|\boldsymbol{S}_{\rm R}|$ (left) and $|\boldsymbol{S}_{\rm T}|$ (right) on (a) $z = 0.0$ slice and (b) $z = -1.5$ slice

References

[1] M. J. Rees, Q. Jl R. Astr. Soc. **28**, 197 (1987).
[2] S. M. Mahajan and Z. Yoshida, Phys. Rev. Lett. **105**, 095005 (2010).
[3] S. M. Mahajan and Z. Yoshida, Phys. Plasmas **18**, 055701 (2011).
[4] S. Mondal et al., PNAS **109**, 8011 (2012).
[5] R. Donat et al., J. Comp. Phys. **146**, 58 (1998).